

ciated with either defective phages or phages altered in host range. We were unable to isolate any plaque-forming units from the EntA⁺ strain MJB234, which carries DNA homologous to phage PS42-D. This may be the reason that *entA*-converting phages could not be identified in two strains previously examined (5, 6).

Our results show that a gene for a *S. aureus* toxin is correlated with phage DNA in all strains examined. Although Blair and Carr (13) demonstrated that the ability to produce α -toxin could be acquired by two of three nontoxigenic strains after lysogenization by the phage L2043, this phage may encode either a regulatory or a structural gene for α -toxin. However, for a different strain, no biochemical evidence for prophage involvement with α -toxin synthesis was obtained (14). The significance of the observation (15) that *S. aureus* strains associated with toxic shock syndrome may have a common temperate phage is unclear; Kreiswirth *et al.* (16) were unable to demonstrate an association between the presence of phage and toxic shock syndrome exotoxin production. These conflicting observations may be due to the respective toxin-converting phages being highly polymorphic in properties such as viability and host range.

There are examples of other bacterial species carrying phages that determine toxin production. The structural genes for diphtheria toxin (17), erythrogenic toxin of *Streptococcus pyogenes* (18), the structural or regulatory genes of botulinum toxins C₁ and D (19), and the shiga-like toxin of *Escherichia coli* (20) are all encoded by temperate phage. How nontoxigenic phages initially acquired toxin genes is unknown. The diphtheria toxin gene (21) and the *entA* gene are both located near the phage attachment site on the genomes of their respective converting phages (Fig. 2). Perhaps the *entA*-converting phage formed as a result of an imprecise excision event between a chromosomal enterotoxin gene and a closely inserted nontoxigenic prophage, as proposed by Laird and Groman for diphtheria toxin (21). Consistent with this hypothesis is our observation that there exist phages that lack the *entA* gene but are related to the *entA*-converting phages. Recombination between these various types of phages may provide a mechanism for the formation of new *entA*-converting phages that have increased host range, or possibly enterotoxin genes with different serological, structural, and biological properties.

References and Notes

1. M. S. Bergdoll, in *Food-borne Infections and Intoxications*, H. Riemann and F. L. Bryan, Eds. (Academic Press, New York, 1979), pp. 443-493.
2. P. A. Pattee and B. A. Glatz, *Appl. Environ. Microbiol.* **39**, 186 (1980).
3. D. H. Mallone, B. A. Glatz, P. A. Pattee, *ibid.* **43**, 397 (1982).
4. M. J. Betley *et al.*, *Proc. Natl. Acad. Sci. U.S.A.* **81**, 5197 (1984).
5. E. P. Casman, *Ann. N.Y. Acad. Sci.* **128**, 124 (1965).
6. A. W. Jarvis and R. C. Lawrence, *Infect. Immun.* **4**, 110 (1971).
7. Strain ISP456 is the restriction-deficient mutant 80 CR3 described by E. E. Stobberingh and K. C. Winkler [*J. Gen. Microbiol.* **99**, 359 (1977)].
8. The plasmid pMJB38 is a pBR322 recombinant plasmid that contains a 623-bp fragment derived from DNA internal to the *entA* structural gene as determined by sequence analysis.
9. A. M. Campell, *Adv. Genet.* **11**, 101 (1962).
10. Analysis of Southern blots with enzyme digests of whole cell DNA from MJB233 and PS42-D DNA that had been hybridized to ³²P-labeled pMJB38 was consistent with the interpretation that whole cell DNA from MJB233 contained both linear and prophage DNA molecules and that the *entA* gene was located near one of the prophage-bacterial junctions. The DNA's were each digested with the following enzymes: Bgl I, Mlu I, Pst I, Sal AI, Bgl I-Mlu I, Bgl I-Pst I, Bgl I-Sal AI, Mlu I-Pst I, and Pst-Sal AI.
11. The phage FR1337-1 was shown to encode the *entA* gene on a 2.5-kb Hind III fragment by Southern blot hybridization with pMJB38 as probe.
12. MJB234 is an EntA⁺ erythromycin-resistant (Erm^r) transformant of FR1710 (EntA⁺, erythromycin-sensitive) whose relevant portion of the *pur-ily* region is substituted with DNA from ISP546 (EntA⁻ Erm^r). MJB164 (EntA⁻; purine, isoleucine, and valine prototroph) is a transformant of ISP484 (EntA⁺; purine, isoleucine, and valine auxotroph) that contains FR1710's *pur-ily* region (4).
13. J. E. Blair and M. Carr, *J. Bacteriol.* **82**, 984 (1961).
14. C. W. Hendricks and R. A. Altenbern, *Can. J. Microbiol.* **14**, 1277 (1968).
15. S. C. Schutzer, V. A. Fischetti, J. B. Zabriskie, *Science* **220**, 316 (1983).
16. B. N. Kreiswirth *et al.*, *Nature (London)* **305**, 709 (1983).
17. L. Barksdale, L. Garmise, R. Rivera, *J. Bacteriol.* **81**, 527 (1967); J. Murphy, A. M. Pappenheimer, Jr., S. T. de Broms, *Proc. Natl. Acad. Sci. U.S.A.* **71**, 11 (1974).
18. J. B. Zabriskie, *J. Exp. Med.* **119**, 761 (1974); C. R. Weeks and J. J. Ferretti, *Infect. Immun.* **46**, 531 (1984).
19. K. Inoue and H. Iida, *C. Jpn. J. Microbiol.* **14**, 87 (1970); *Jpn. J. Med. Sci. Biol.* **24**, 53 (1971).
20. A. D. O'Brien *et al.*, *Science* **226**, 694 (1984).
21. R. K. Holmes, *J. Virol.* **19**, 195 (1976); W. Laird and N. Groman, *ibid.*, p. 208; *ibid.*, p. 228; R. K. Holmes and L. Barksdale, *ibid.* **3**, 586 (1969).
22. Modifications of the DNA-DNA hybridization procedure [E. Southern, *J. Mol. Biol.* **98**, 503 (1975)] have been described [J. J. Mekalanos, *Cell* **35**, 253 (1983)].
23. T. Maniatis, A. Jeffrey, D. G. Kleid, *Proc. Natl. Acad. Sci. U.S.A.* **72**, 1184 (1975).
24. M. L. Stahl and P. A. Pattee, *J. Bacteriol.* **154**, 395 (1983).
25. N. E. Thompson and P. A. Pattee, *ibid.* **148**, 294 (1981).
26. R. W. Davis, D. Botstein, J. R. Roth, *Advanced Bacterial Genetics—A Manual for Genetic Engineering* (Cold Spring Harbor Laboratory, Cold Spring Harbor, N.Y., 1980), pp. 109-111.
27. We thank G. A. Hancock, W. J. van Leeuwen, A. W. Jarvis, and P. A. Pattee for providing bacterial strains. Supported by a Damon Runyon-Walter Winchell Cancer Fund fellowship, DRG-733 (M.J.B.).

15 February 1985; accepted 15 May 1985

Localized Control of Ligand Binding in Hemoglobin: Effect of Tertiary Structure on Picosecond Geminate Recombination

Abstract. *The picosecond geminate rebinding of molecular oxygen was monitored in a variety of different human, reptilian, and fish hemoglobins. The fast (100 to 200 picoseconds) component of the rebinding is highly sensitive to protein structure. Both proximal and distal perturbations of the heme affect this rebinding process. The rebinding yield for the fast process correlates with the frequency of the stretching motion of the iron-proximal histidine mode (ν_{Fe-His}) observed in the transient Raman spectra of photodissociated ligated hemoglobins. The high-affinity R-state species exhibit the highest values for ν_{Fe-His} and the highest yields for fast rebinding, whereas low affinity R-state species and T-state species exhibit lower values of ν_{Fe-His} and correspondingly reduced yields for this geminate process. These findings link protein control of ligand binding with events at the heme.*

J. M. FRIEDMAN
T. W. SCOTT*
G. J. FISANICK
AT&T Bell Laboratories,
Murray Hill, New Jersey 07974
S. R. SIMON
Department of Biochemistry,
State University of New York,
Stony Brook 11794
E. W. FINDSEN
M. R. ONDRIAS
Department of Chemistry,
University of New Mexico,
Albuquerque 87106
V. W. MACDONALD
Department of Hematology,
Johns Hopkins Medical Center,
Baltimore, Maryland 21205

Hemoglobin (Hb) reactivity toward ligands such as O₂ or CO is characterized by macroscopic measurements of ligand binding ("on" rates) and ligand dissociation ("off" rates). These parameters of reactivity are highly responsive to protein structure. One acquires coarse control of the reactivity by changing the quaternary structure. The two well-defined quaternary structures of hemoglobin (1, 2), termed the R state and T state, exhibit, respectively, enhanced and reduced reactivity toward these ligands (1). Fine tuning of the reactivity can occur through solution-induced or spe-

*Present address: Corporate Research Science Laboratories, Exxon Research Laboratories, Annandale, N.J. 08801.

cies-specific variations in the properties of these quaternary structures (3–6). The microscopic details of how changes in protein structure modulate the on and off rates remain an important and as yet unanswered question in biophysics.

It was recently shown that for each quaternary structure there are two spectroscopically well-defined, tertiary struc-

tures of the protein environment about the heme corresponding to the state of ligation (4–6). Within both quaternary structures, ligand binding induces localized changes about the heme, giving rise to both a ligated R and a ligated T tertiary structure. Upon ligand dissociation the ligated R(T) begins to relax to the deoxy R(T) geometry. For the R

state of HbA, this pH-sensitive relaxation can occur within a fraction of a microsecond after dissociation (7). Consequently, macroscopic rate constants that are measured over comparable or longer time periods cannot necessarily be assigned to a fixed average configuration. Similarly, the affinity is a measure of the binding properties of the R and T structures and of the saturation-dependent equilibrium constant for the two structures. Thus, none of the standard macroscopic parameters of reactivity can be adequately correlated with the microscopic structural details of a specific tertiary configuration of a given Hb molecule.

After the rupture of the heme-ligand bond, the ligand can either rebind from within the protein (termed geminate recombination) or can escape into the surrounding solvent. Geminate recombination occurs for hemoglobin and myoglobin from within a few picoseconds to ~100 nsec after ligand dissociation (8–14). On the subnanosecond time scale, the protein structure surrounding the dissociated ligand-heme complex should closely resemble that of the parent ligated species, with only slight modifications of the protein to accommodate the rapid movement of iron out of the plane of the heme. Recent picosecond Raman experiments in our laboratory (15) revealed that the peak frequencies in the Raman spectra of both R- and T-state photolyzed carboxy Hb (COHb) do not evolve between 20 psec and 10 nsec after photolysis. Virtually all hemoglobins have the same porphyrin chromophore to which the ligand rebinds. Thus, for a given ligand, differences in the subnanosecond geminate rebinding must therefore be attributable to differences at the heme originating from the protein. Geminate recombination provides the opportunity of directly studying the influence of protein structure upon the most elementary kinetic event associated with ligand binding. In this study we examined how both quaternary and tertiary structures influence geminate rebinding on the subnanosecond time scale. Hemoglobins studied included those from adult humans (HbA), the Javan wart snake (*Acrochordus javanicus*), swordfish, carp, Ridley sea turtle (*Lepidochelys kempfi*), leatherback turtle (*Dermochelys coriaca*), and the mutant human hemoglobins Hb (Zürich) (HbZ) and Hb (Kempsey) (HbK).

The geminate recombination of CO in HbA and of O₂ in HbA and HbZ at pH 8.2 is shown in Fig. 1. It is possible to assign these single-frequency (435 nm) decay curves to geminate recombination

Fig. 1. Comparison of the geminate recombination of carboxy HbA (COHbA), oxy HbA (O₂HbA), and oxy Hb (Zürich) (O₂HbZ) at pH 8.2 (~10°C). Concentration refers to the relative concentration of deoxy heme computer-generated from the initial time-dependent transmission curves. Geminate recombination was studied with single 30-psec pulses at the second harmonic (532 nm) of an active passive mode-locked Nd³⁺: yttrium-aluminum-garnet laser (Quantel YG 471C) operating at 10 Hz to photolyze a ligated hemoglobin sample in a cell with a 1-mm path length at ~10°C. The Hb concentration was sufficiently low (~2 to 3 × 10⁻⁴M) that absorption at the photolyzing wavelength was negligible, so that uniform concentration of excited species through the cell path could be assumed. The recombination was monitored by probing the transmission of attenuated blue pulses (436 nm) of ~25-psec duration generated by passing the second harmonic through a hydrogen cell (300 pounds per square inch). The blue pulse results from the first anti-Stokes Raman transition. The time between pump and probe pulses was varied with a programmable optical delay line (Klinger), providing delays of up to 2.4 nsec. Because of the high pulse-to-pulse stability (≤5 percent), it was possible to generate the rebinding curve by slowly varying the delay line distance. The reproducibility was sufficiently good to allow for signal averaging (repetitive scans) when necessary. The transmission was monitored by a fast photodiode screened with appropriate optical filters. The output of this photodiode and another that monitored the incident pulse energies were averaged in a boxcar integrator and the ratio was taken to compensate for pulse-to-pulse variations. The output of the boxcar averager was digitized and stored in a computer. Computer-controlled shutters provided a base-line value for the transmission of the sample in the absence of the photolysis pulse. The curves were converted to absorbance and displayed as relative concentration of deoxyheme versus delay. The pulses were characterized by slowly scanning the rise time of the transmission change which is known to be subpicosecond (11, 12). The samples were prepared by the method of Huisman and Dozy (29).

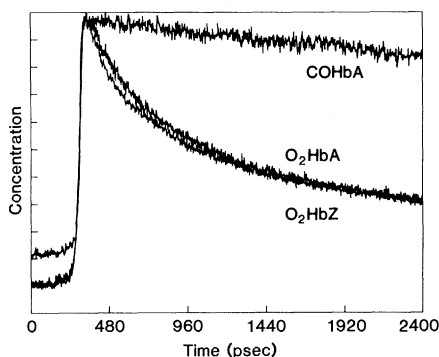


Table 1. Comparison for several hemoglobins of the subnanosecond geminate yield (GY, the relative geminate yield for O₂ at 1 nsec after photolysis with a 30-psec green pulse) with specific structural features. The GY values are an indication of the relative magnitudes of the fast 200-psec component of the geminate rebinding process. The values of $\nu_{\text{Fe-His}}$ [from (4–6)] refer to the frequency (in reciprocal centimeters) of the iron-proximal histidine stretching mode in the deoxy transients occurring within 10 nsec of photolysis. The spontaneous off rates (*K*) for HbA and Hb (*Acrochordus javanicus*) are also shown. The off rates determinations and the assignment of quaternary structure (QS) for Hb (*Acrochordus*) were made in the laboratory of one of us (S.R.S.). The asterisk indicates that for the GY measurement but not the Raman measurement the sample was not stripped of organic phosphates. Consequently, the 50 percent value for GY is a lower limit. The GY value for myoglobin was obtained in another laboratory with femtosecond pulses (19). Hemoglobin abbreviations: A, adult human; Z, Zürich; K, Kempsey; SF, swordfish; Lk, *Lepidochelys kempfi* (Ridley turtle); Dc, *Dermochelys coriaca* (leatherback turtle); Aj, *Acrochordus javanicus* (Javan wart snake or elephant trunk snake).

Protein	GY (%)	$\nu_{\text{Fe-His}}$	<i>K</i> (sec ⁻¹)	QS
HbA, pH 8.2	70	230	10	R
HbK, pH 8.2	70	230		R
HbZ, pH 8.2	75	230		R
Hb (Aj), pH 8.2*	50	230	<50	R
HbA, pH 6 + IHP	40	228	100	R
HbK, pH 6 + IHP	40	228		R
Hb (SF), pH 8.2	10	225		R
Hb (carp), pH 8.2	10	224		R
Hb (Lk), pH 8.2	10	223		R
Hb (Dc), pH 8.2	10	223		R
Hb (Aj), pH 6 + IHP	5	220	750	T
Myoglobin	5	222		

and not structural relaxation for several reasons. The Raman spectra of the photodissociated species, which should be sensitive to structural relaxation, shows no evolution of peak frequencies from ~ 25 psec to 10 nsec after photolysis (15). In addition, the transient Raman spectra of photolyzed CO- and O₂-saturated HbA are identical over the time course in Fig. 1, even though CO rebinding is substantially less than O₂ rebinding on this time scale for both HbA and HbZ (16). The decay curves in Fig. 1 are also very similar to those generated from the full transient absorption spectrum (9). Figure 1 shows the biphasic nature of O₂ rebinding. The fast (~ 200 psec) component evident in the O₂ rebinding kinetics is absent for CO rebinding. Increasing the temperature to $\sim 35^\circ\text{C}$ decreased the proportion of the fast component relative to the slower rebinding process. These decay curves reveal that both O₂ and CO exhibit a slower rebinding, which begins on a subnanosecond time scale and persists to the nanosecond regime. It appears likely that this latter process evolves smoothly into the ~ 100 -nsec lifetime rebinding observed for both CO and O₂ (8, 14). The fast O₂ rebinding is highly nonexponential, whereas the slower rebinding appears more nearly exponential for both O₂ and CO. It is plausible that these fast and slow components correspond to Frauenfelder's processes 1 and M, respectively (17, 18).

We examined the slight difference between HbA and HbZ in the fast component of the rebinding seen in Fig. 1 more closely in an expanded scan covering only the first few hundred picoseconds. HbZ reproducibly shows slightly faster decay at the earliest times. Figure 2 depicts the effect of lowering the pH and adding inositol hexaphosphate (IHP) on the geminate rebinding of O₂ for HbA and Hb (*Acrochordus*). In both instances the low pH conditions are associated with a decrease in the magnitude of the fast component of the rebinding with the *Acrochordus* sample showing a more pronounced effect. Solutions of HbK at high and low pH yielded results comparable to those of HbA. Hb samples from the swordfish, carp, Ridley turtle, and leatherback turtle gave geminate rebinding curves at pH 8.2 with little evidence of the fast components. The resulting curves appeared relatively flat as compared to those from HbA, HbZ, HbK, and Hb (*Acrochordus*) (Table 1).

Recent femtosecond studies (19) demonstrated that for O₂ the 100- to 200-psec rebinding is the first rebinding process occurring after dissociation. Our findings leave little doubt that the induced

changes in this process originate from structural differences at or very near the heme, as suggested from cryogenic studies (17, 20). All the comparisons shown in Figs. 1 and 2 involve known differences in the tertiary structure. HbZ differs from HbA in that the distal histidine of the β subunit is replaced by an arginine. This substitution alters the distal environment about the heme (21). Studies of the geminate rebinding of CO in both the intact tetramer (16, 20, 21) and the isolated β subunits (18) reveal that, relative to HbA and its β subunits, there is both a faster geminate rebinding and a lower inner barrier for rebinding. Raman studies (16) show that functionally important regions of the proximal environment are roughly the same for HbA and HbZ, as reflected in the frequency of the iron-proximal histidine ($\nu_{\text{Fe-His}}$) stretching mode.

In contrast to the case for HbA versus HbZ, where a significant distal perturbation only modestly affects the geminate yield for O₂, the substantial solution-induced changes (Fig. 2) appear related to the proximal environment. Recent picosecond Raman studies indicate that the values for $\nu_{\text{Fe-His}}$ (Table 1) apparent at 10 nsec are already fully developed by ~ 25 psec after dissociation (15). Solution conditions that decrease $\nu_{\text{Fe-His}}$ also cause a decrease in the subnanosecond geminate yield that appear to scale with

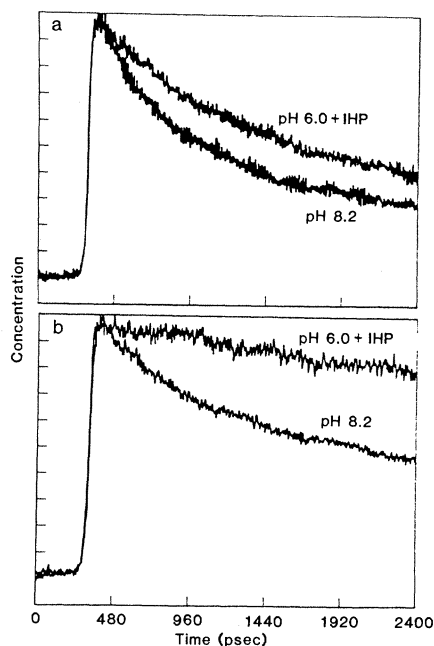


Fig. 2. Comparison of the geminate rebinding of O₂ as a function of pH for (a) HbA and (b) Hb (*Acrochordus*). All samples of Hb used in this study except Hb (*Acrochordus*) were initially stripped of the intrinsic phosphates. Inositol hexaphosphate concentrations were typically 3 mM in bis tris buffer. Tris buffer was used for the samples at pH 8.2.

$\Delta\nu_{\text{Fe-His}}$ (Table 1). For example, in going from pH 8.2 to pH 6.0 + IHP, O₂ Hb (*Acrochordus*) undergoes a change in quaternary structure (22). Under these conditions the value of $\nu_{\text{Fe-His}}$ drops from ~ 230 to ~ 220 cm⁻¹, and the magnitude of the prominent fast component of the geminate rebinding curve (Fig. 2) seen at pH 8.2 essentially vanishes. Although this change in solution condition does not cause a change in the quaternary structure for O₂ HbA (23), there are indications from the absorption spectrum (23) and the Raman spectrum (6, 7) that the ligated R structure is destabilized in the direction of the T structure. For both O₂ and CO, this destabilization is reflected in the transient species by a decrease in $\nu_{\text{Fe-His}}$ (230 to 228 cm⁻¹) that is smaller in magnitude but in the same direction as that observed for a transition from the R to the T state. Similarly, the decrease in the magnitude of the last geminate process is also correspondingly reduced compared to Hb (*Acrochordus*). A comparison at pH 8.2 of Hb's from different sources indicates that variation in the proximal environment (as reflected in $\nu_{\text{Fe-His}}$) is linked to species-specific differences in the geminate yield. Those Hb's that have the lower values for $\nu_{\text{Fe-His}}$ exhibit a reduced magnitude for the 200-psec component (Table 1). Because species-specific differences in the distal environment can also influence the geminate yield, the correlation between $\nu_{\text{Fe-His}}$ and geminate yield is not expected to be totally rigorous for interspecies comparisons.

In earlier studies (4-6) it was shown that solution-induced changes in the yield of photolysis averaged over a 10-nsec pulse correlated with changes in protein structure as reflected in $\nu_{\text{Fe-His}}$. A dependence on protein structure for geminate rebinding was also inferred for the quantum yield of photolysis for O₂Hb averaged over 350-nsec pulses (24). Our work indicates that the correlation extends directly to the picosecond geminate rebinding. In view of the time scale for the geminate process and the close association with $\nu_{\text{Fe-His}}$, there can be little doubt that the innermost potential barrier controlling ligand binding (17) is affected to a substantial degree by protein-induced changes in the iron-proximal histidine linkage. It has been argued that the variation in $\nu_{\text{Fe-His}}$ originates from variations in the tilt of the histidine (in its own plane) with respect to the heme plane (5-7). This claim, in conjunction with the above correlations between $\nu_{\text{Fe-His}}$ and the geminate yield, strongly supports models for protein control of ligand binding (6, 7, 25-27)

based on a quaternary structure-dependent tilt of the proximal histidine with respect to the heme. Karplus and co-workers (26) pointed out the potential significance of this tilt on the basis of theoretical analysis of the x-ray crystallographic studies of Baldwin and Chothea (28).

References and Notes

1. M. F. Perutz, *Proc. R. Soc. London Ser. B* **208**, 135 (1980).
2. R. G. Shulman, J. J. Hopfield, S. Ogawa, *Q. Rev. Biophys.* **8**, 325 (1975).
3. A. DeYong *et al.*, *J. Biol. Chem.* **251**, 6692 (1976); L. D. Kwiatowski and R. W. Noble, *ibid.* **257**, 8891 (1982).
4. J. M. Friedman, R. A. Stepnoski, R. W. Noble, *FEBS Lett.* **146**, 278 (1982); T. W. Scott *et al.*, *ibid.* **158**, 68 (1983).
5. J. M. Friedman *et al.*, *Science* **218**, 1244 (1982); J. M. Friedman, *Time-Resolved Vibrational Spectroscopy*, G. Atkinson, Ed. (Academic Press, New York, 1983), p. 307.
6. J. M. Friedman *et al.*, *J. Biol. Chem.* **258**, 10564 (1983).
7. T. W. Scott and J. M. Friedman, *J. Am. Chem. Soc.* **106**, 5677 (1984).
8. D. A. Duddell, R. J. Morris, J. T. Richards, *Chem. Commun.* **1979**, 75 (1979); B. Alpert *et al.*, *Chem. Phys. Lett.* **64**, 11 (1979); J. M. Friedman and K. B. Lyons, *Nature (London)* **284**, 570 (1980); D. A. Duddell *et al.*, *Photochem. Photobiol.* **31**, 479 (1980).
9. P. A. Cornelius *et al.*, *Proc. Natl. Acad. Sci. U.S.A.* **78**, 7526 (1981).
10. D. A. Chernoff, R. M. Hochstrasser, A. W. Steele, *ibid.* **77**, 5606 (1980); D. A. Chernoff, R. M. Hochstrasser, A. W. Steele, in *Hemoglobin and Oxygen Binding*, C. Ho, Ed. (Elsevier-North Holland, New York, 1982), pp. 245-350; P. A. Cornelius and R. M. Hochstrasser, *Springer Ser. Chem. Phys.* **23**, 288 (1982).
11. J. L. Martin *et al.*, *Biochem. Biophys. Res. Commun.* **107** (No. 3), 803 (1982).
12. J. L. Martin *et al.*, *Springer Ser. Chem. Phys.* **23**, 294 (1982).
13. J. H. Hoffrichter, E. R. Henry, W. A. Eaton, *Proc. Natl. Acad. Sci. U.S.A.* **80**, 2235 (1983).
14. E. R. Henry *et al.*, *J. Mol. Biol.* **166**, 443 (1983).
15. E. W. Finsen *et al.*, *Science*, in press.
16. T. W. Scott, J. M. Friedman, V. W. MacDonal, *J. Am. Chem. Soc.*, in press.
17. W. Doster *et al.*, *Biochemistry* **21**, 4831 (1982); R. H. Austin *et al.*, *ibid.* **14**, 5355 (1975).
18. D. D. Dlott *et al.*, *Proc. Natl. Acad. Sci. U.S.A.* **80**, 623 (1983).
19. J. L. Martin, personal communication.
20. M. R. Ondrias *et al.*, *Chem. Phys. Lett.* **112**, 351 (1984).
21. S. E. V. Phillips, D. Halle, M. F. Perutz, *J. Mol. Biol.* **150**, 137 (1981); K. H. Winterhalter *et al.*, *Eur. J. Biochem.* **11**, 435 (1969); P. W. Tucker *et al.*, *Proc. Natl. Acad. Sci. U.S.A.* **75**, 1076 (1978); G. M. Giacometti *et al.*, *J. Biol. Chem.* **255**, 6160 (1980).
22. J. M. Friedman, S. R. Simon, T. W. Scott, *Copeia*, in press.
23. M. F. Perutz *et al.*, *Biochemistry* **15**, 8 (1976).
24. R. J. Morris and Q. H. Gibson, *J. Biol. Chem.* **259**, 367 (1984).
25. J. M. Friedman and T. W. Scott, in *Hemoglobins: Structure and Function*, A. G. Schneck, Ed. (Brussels Univ. Press, Brussels, 1983), pp. 269-284; J. M. Friedman, *Science*, in press.
26. B. R. Gelin and M. Karplus, *Proc. Natl. Acad. Sci. U.S.A.* **74**, 801 (1977).
27. B. R. Gelin, A. W.-M. Lee, M. Karplus, *J. Mol. Biol.* **171**, 489 (1983).
28. J. M. Baldwin and C. Chothea, *ibid.* **129**, 175 (1979).
29. T. H. Huisman and A. M. Dozy, *J. Chromatogr.* **19**, 160 (1965).
30. M.R.O. acknowledges the financial support of the National Institutes of Health (grants I R01 GM 33330-1 and DHHS2-S06 RR08139), the donors of the Petroleum Research Fund as administered by the American Chemical Society, and the University Research Support Program of Sandia National Laboratories. We thank R. Noble and F. Bunn for samples of Hb (carp) and Hb (Kempsey), respectively; P. Lutz and W. Friar for assistance in drawing blood samples from assorted reptiles; J. L. Martin for sharing unpublished data with us.

Expression of Two Variant Surface Glycoproteins on Individual African Trypanosomes During Antigen Switching

Abstract. *Individual Trypanosoma brucei rhodesiense organisms were observed in the process of switching variant surface glycoproteins (VSG's). During this switch, trypanosomes simultaneously expressed both pre- and postswitch VSG's uniformly over their surface as detected with monoclonal antibodies. Analysis of this switching event showed that trypanosomes expressing any one of three distinct preswitch VSG's could switch to expression of from one to three different postswitch VSG's. Up to 2.7 percent of the trypanosome population was in the process of switching at one time.*

KLAUS M. ESSER

MAURICE J. SCHOENBECHLER

Department of Immunology, Walter Reed Army Institute of Research, Washington, D.C. 20307-5100

African trypanosomes undergo frequent gene switching events that result in major phenotypic changes observable as antigenic variation (1-4). This antigenic variation is manifested by expression of a series of immunologically distinct variant surface glycoprotein (VSG) coats on trypanosomes during the course of infection in mammalian hosts. Each of these VSG's is produced through selective expression of one of several hundred VSG genes within the genome of individual trypanosomes (5). The precise mechanism whereby one VSG gene is selected for transcription in a trypanosome at a given time is unknown, although genomic DNA rearrangements are apparently involved (6).

Studies of differential gene expression in trypanosomes are hampered by a major drawback of the system. It has not been possible to observe actual switching events or to determine precise pre- and postswitch trypanosome phenotypes. We have, however, found a time during trypanosome infection when the switch from expression of one VSG gene to another occurs naturally in most of the parasites. This high switch frequency, together with a relatively high parasitemia in experimental animals at the time of the switch, has permitted us to examine specific events of antigenic variation.

Variant antigen type (VAT) switching occurs at a high frequency during the initial parasitemia in mice inoculated with *Trypanosoma brucei rhodesiense* in the metacyclic stage (obtained from the salivary glands of laboratory-reared tsetse flies) (Fig. 1). Trypanosomes in the early blood stage initially continue to express all metacyclic-variant antigen

Table 1. Percentage of MVAT-expressing trypanosomes that also expressed the indicated BVAT's in a BALB/cJ mouse inoculated with metacyclic trypanosomes from tsetse flies infected with WRATat 1.10. Direct immunofluorescence reactions on live trypanosomes were carried out as described in the legend of Fig. 2 for trypanosomes collected from one mouse on days 4 through 7 of infection. Similar results were obtained in other mice inoculated with metacyclic trypanosomes derived from WRATat 1.1 or 1.14 (as described in the legend of Fig. 1), although the highest percentage of double-labeled trypanosomes occurred in mice inoculated with metacyclic trypanosomes derived from WRATat 1.10 or 1.14. No double-labeled trypanosomes were observed before day 4 or after day 6 of infection in any of the mice.

MVAT number*	Percentage of MVAT's†	BVAT specificity (percent)‡		
		WRATat 1.1	WRATat 1.14	WRATat 1.10
<i>Day 4 of infection</i>				
4	10	0	0	0
6	49	0.15	0.23	0
7	30	0.4	0.7	1.2
<i>Day 5 of infection</i>				
4	5	0	3.7	0
6	33	1.5	1.7	0
7	16	3.9	5.0	0
<i>Day 6 of infection</i>				
4	1	0	0	0
6	1	0	0	0
7	4	1.5	10.5	3.8

*All VAT's are mutually exclusive (7, 15, 16, 18), and each is defined by a monoclonal antibody: MVAT's 4, 6, and 7 by antibodies 3.2C5.2, 3.2C2.2, and 3.103.1, respectively; and BVAT's 1.1, 1.14, and 1.10 by antibodies 12.4F3.1, 21-14-146D, and 59-10-92J, respectively. †Values indicate the percentage of trypanosomes expressing each MVAT at the time of assay for dual expression. ‡Values are percentages of trypanosomes reactive with monoclonal antibodies specific for the indicated MVAT's that also reacted with a monoclonal antibody specific for a BVAT. Percentages were calculated on the basis of single counts of 200 to 2000 trypanosomes. Values of zero indicate that the particular switch from MVAT to BVAT was not observed in samples of at least 2000 trypanosomes.